

BULLETIN

OF THE

KOREAN CHEMICAL SOCIETY

VOLUME 16, NUMBER 9
SEPTEMBER 20, 1995

BKCS 16(9) 787-898
ISSN 0253-2964

Communications

Characterization of An Oxygen Species in Copper Oxide-Alumina System

Chong Soo Han* and Hakze Chon†

*Department of Chemistry, Chonnam National University,
Kwangju 500-757, Korea*

*†Department of Chemistry,
Korea Advanced Institute of Science,
Daejeon 305-701, Korea*

Received April 11, 1995

Copper oxide or cuprous oxide is a well known catalyst for oxidation of CO¹ and partial oxidation of propene.²⁻⁶ It is expected that copper oxide transforms oxygen molecule to more reactive species and the oxygen species have important roles in the catalytic processes. EPR is one of the best tools to understand the roles of oxygen species in catalytic oxidations⁷ but the EPR signal of oxygen species adsorbed on copper oxide is not observed yet because of the spin-spin interaction of Cu²⁺ and oxygen species (O₂⁻, O⁻). Another method to identify the oxygen species is capturing the species from copper oxide with a suitable surface which does not react with oxygen molecule, stabilizes oxygen species and does not interfere the observation of the EPR signals. In this study, we chose γ -alumina as a surface stabilizing oxygen species,⁸ and monitored EPR spectrum of copper oxide supported on γ -alumina in oxygen adsorption process.

¹⁶O₂ was Matheson's ultra high purity (99.999%) and CO was high purity grade (99.99%). O₂ enriched with 20% ¹⁷O was obtained from Merck Sharp and Dohme Canada, Ltd.. A Mass spectrometric analysis of O₂ enriched with 20% ¹⁷O showed a composition of 16.7% ¹⁶O¹⁶O, 20.7% ¹⁷O¹⁶O, 31.2% ¹⁶O¹⁸O, 0.5% ¹⁷O¹⁷O, 18.6% ¹⁷O¹⁸O and 12.8% ¹⁸O¹⁸O. Cylindrical particles of γ -alumina (specific surface area: 90 m²/g) were impregnated with an aqueous solution of copper nitrate (99.9995%, Johnson Matthey Chemicals, Ltd.). They were dried and calcined in air at 873 K for 5 hr. Cuprous oxide or copper-rich cuprous oxide sample was obtained by heating the calcined sample in CO at 973 K for 2 hr. The copper concentration of the sample was about 5 wt%. The EPR mea-

surement was carried out using an X band spectrometer at 77 K. The *g*-values and relative intensities were calculated by comparing the *g*-value and integrated area of the DPPH signal. The EPR sample tube (diameter: 3 mm) was connected by a Teflon union to a conventional high vacuum apparatus which was maintained at 1.3×10⁻⁶ Pa. The tube with stopcock could be easily detached or connected to the vacuum system.

γ -Alumina after treatment with O₂ or CO at 298-773 K showed no EPR signal in the range *g*=2.4-1.7. Copper oxide supported on alumina treated with CO at 973 K for 2 hr showed no EPR spectra in the range *g*=2.4-1.7 indicating the sample was reduced to cuprous oxide or copper-rich cuprous oxide.

When the reduced sample was oxidized in 3.3×10⁴ Pa ¹⁶O₂ for 2 hr at 773 K, the EPR spectrum of Cu²⁺ with *g*=2.05, 2.33 appeared. The *g* values of Cu²⁺ were consistent with that of Cu²⁺ observed by Berger and Roth.⁹ The observed spin concentration was 1.3×10²⁰ spin/g which corresponds to 30% of the total copper present.

When the cuprous oxide or copper-rich cuprous oxide supported on alumina was treated with 6.7×10³ Pa ¹⁶O₂ for 20 min. at 298 K, an asymmetric signal (Signal A) was produced together with the signal due to Cu²⁺ as shown in Figure 1. The concentrations of Cu²⁺ and Signal A was 8×10¹⁷ spin/g and 8×10¹⁷ spin/g, respectively. When ¹⁶O₂ was admitted at 373 K, the intensity of Signal A decreased while that of Cu²⁺ increased (Signal A: 6×10¹⁷ spin/g, Cu²⁺: 2×10¹⁸ spin/g). When the sample was treated with ¹⁶O₂ at 473 K, the decrease in Signal A and increase in the intensity of Cu²⁺ signal were larger compared with the treatment at 373 K (Signal A: 3×10¹⁷ spin/g, Cu²⁺: 6×10¹⁸ spin/g). Signal A was not observed however, when ¹⁶O₂ was admitted to the sample at 573 K. Heating the sample at 473 K treated previously with ¹⁶O₂ at 298 K resulted in a decrease in Signal A and an increase in Cu²⁺ signal. Signal A was characterized by *g*₁=2.035, *g*₂=2.010, *g*₃=2.004 with a super hyperfine structure as shown in Figure 2. The superhyperfine splittings for *g*₂ and *g*₃ were 3.8±0.2 G in both, while that of *g*₁ was not clear.

Figure 3 shows the EPR spectrum of the sample when O₂ enriched with 20% ¹⁷O was admitted at 298 K. Signal

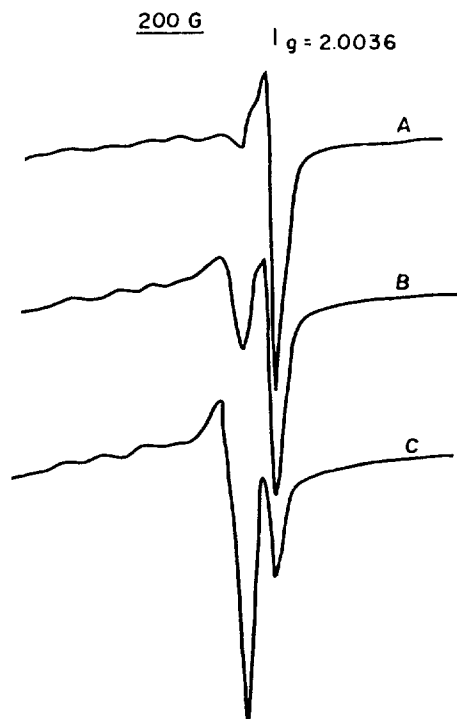


Figure 1. EPR spectra of $^{16}\text{O}_2$ adsorbed on reduced copper oxide- γ -alumina at 77 K. Sample was exposed to 6.7×10^3 Pa $^{16}\text{O}_2$ for 20 min at 298 K: A; 373 K: B; 473 K: C.

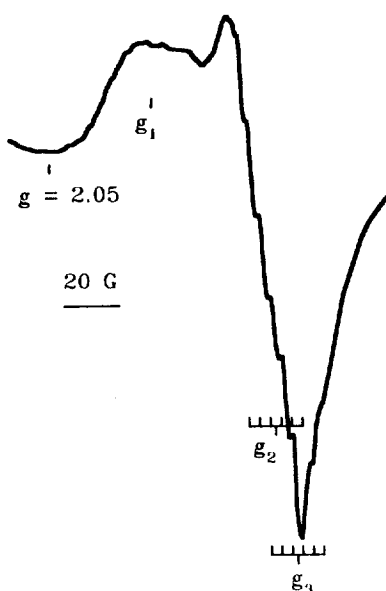


Figure 2. Expanded EPR spectrum of $^{16}\text{O}_2$ adsorbed on reduced copper oxide- γ -alumina at 77 K. Sample was exposed to 6.7×10^3 Pa $^{16}\text{O}_2$ for 20 min at 298 K.

A showed two sets of hyperfine structure with 6 lines ($I=5/2$) separated by 117 ± 1 G and 28 ± 0.5 G respectively. Both sets were centered about g_3 . Hyperfine due to $^{17}\text{O}^{17}\text{O}$ was not observed because of its low concentration.

Signal A appeared when O_2 was admitted to the cuprous oxide or copper-rich cuprous oxide at low temperature. The development of two sets of hyperfine splitting centered on

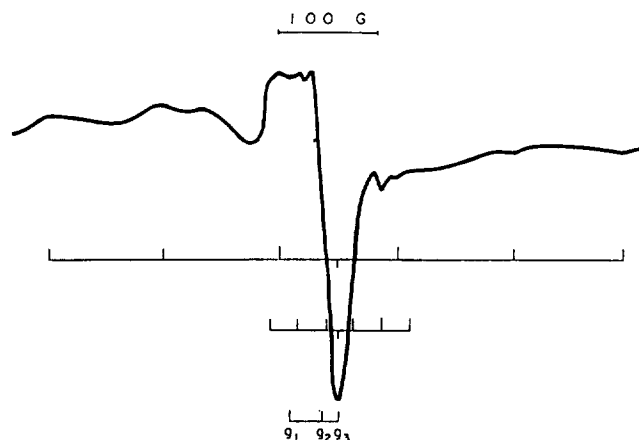


Figure 3. EPR spectrum of $^{17}\text{O}_2$ adsorbed on reduced copper oxide- γ -alumina at 77 K. Sample was exposed to 6.7×10^3 Pa O_2 enriched with 20% ^{17}O for 20 min at 298 K.

g_3 component when treated with O_2 enriched with 20% ^{17}O implies that two or more oxygen atoms lie along a principle axis. The total spin density of two different oxygen atoms was 0.97.¹⁰ Signal A, therefore, may originate from O_2^- . Signal A showed a super hyperfine splitting indicating an interaction of the radical with a nucleus with $I=5/2$. The fact and the value of g_1 , 2.035, suggest that O_2^- is adsorbed on Al^{3+} of the surface.⁷ The g values of signal A are close to that of O_2^- on Al^{3+} of AlSb ,¹¹ γ -irradiated alumina,¹² zeolite Y,¹³ and alumina supported molybdenum.¹⁴ The unequal hyperfine splitting of $^{17}\text{O}^{16}\text{O}$ or $^{17}\text{O}^{18}\text{O}$ in the case of signal A suggests that the molecular axis of O_2^- is not parallel to the surface, *i.e.*, a peroxy type O_2^- .¹⁵

When O_2 was admitted to the reduced copper oxide, there was always an increase in Cu^{2+} signal together with an increase in O_2^- signal. It indicates that an electron moves from Cu^+ to molecular oxygen. Studies reported that O_2^- was formed on γ -irradiated alumina but the radical was not formed on thermally activated alumina.¹² So we can suggest that $\text{Cu}^{2+}\text{-O}_2^-$ is formed in the adsorption of O_2 on cuprous oxide and a part of O_2^- moves to Al^{3+} showing Cu^{2+} and $\text{Al}^{3+}\text{-O}_2^-$ signals. The situation is similar to the case of molybdenum⁸ or ruthenium¹⁶ supported on γ -alumina. Lumpov and coworkers suggested that the experimentally observed EPR constants in the adsorption of O_2 on $\text{Cu}^{2+}/\text{SiO}_2$ originated from the hypothetical weak complex $(\text{Cu}\cdot\text{O}_2)^{2+}$.¹⁷ In our observation, Signal A grows with Cu^{2+} signal and the formation of $(\text{Cu}\cdot\text{O}_2)^{2+}$ can be excluded.

The fact that an increase in Cu^{2+} signal was observed with a decrease in O_2^- signal when O_2 preadsorbed sample was heated under O_2 ambient as well as under vacuum, suggests the transformation of O_2^- to O_2 by taking electrons from Cu^+ ions.

Acknowledgment. This work was supported by the Korea Science and Engineering Foundation (931-0300-004-2).

References

1. Jernigan, G. C.; Somerjai, G. A. *J. Catal.* **1994**, *147*, 567.
2. Wood, B. J.; Wise, H.; Yolles, R. S. *J. Catal.* **1969**, *15*,

355.

3. Voge, H. H.; Wagner, C. D.; Stevenson, D. P. *J. Catal.* **1963**, *2*, 58.
4. Adams, C. R.; Jennings, T. J. *J. Catal.* **1963**, *2*, 63.
5. Davydov, A. A.; Mikhaltchenko, V. G.; Sokolovskii, V. D.; Boreskov, G. K. *J. Catal.* **1978**, *55*, 299.
6. Shultz, K. H.; Cox, D. F. *J. Catal.* **1993**, *143*, 464.
7. (a) Lunsford, J. H. *Catal. Rev.* **1973**, *8*, 135. (b) Che, M.; Tench, A. J. *Adv. Catal.* **1983**, *32*, 1.
8. Losee, D. B. *J. Catal.* **1977**, *50*, 545.
9. Berger, P. A.; Roth, J. F. *J. Phys. Chem.* **1967**, *71*, 4307.
10. The hyperfine splittings for ^{17}O atoms can be resolved into isotropic parts and anisotropic parts as

$$\begin{bmatrix} 0 \\ 0 \\ -28 \end{bmatrix} = -28/3 + \begin{bmatrix} 28/3 & & \\ & 28/3 & \\ & & -56/3 \end{bmatrix} \text{ and}$$

$$\begin{bmatrix} 0 \\ 0 \\ -117 \end{bmatrix} = -117/3 + \begin{bmatrix} 117/3 & & \\ & 117/3 & \\ & & -234/3 \end{bmatrix}, \text{ respectively.}$$

The total spin density in O_2^- is $(-28/3)/(-1651) + (-28/3)/(-51.38) + (-117/3)/(-1651) + (-117/3)/(-51.38) = 0.97$.^{7b}

11. Miller, D. J.; Haneman, D. *Phys. Rev. B.* **1971**, *3*, 2918.
12. Eley, D. D.; Zammitt, M. A. *J. Catal.* **1971**, *21*, 366.
13. Wang, K. M.; Lunsford, J. H. *J. Phys. Chem.* **1969**, *73*, 2069.
14. Che, M.; McAteer, J. C.; Tench, A. J. *Chem. Phys. Lett.* **1975**, *31*, 145.
15. Ben Taarit, Y.; Lunsford, J. H. *J. Phys. Chem.* **1973**, *77*, 780.
16. Sabbadini, M. G. B.; Gervasini, A.; Morazzoni, F.; Strumulo, D. *J. Chem. Soc., Faraday Trans. 1*, **1987**, *83*, 2271.
17. Lumpov, A. I.; Mikheikin, I. D.; Zhidomirov, G. M.; Kazanski, V. B. *Kinet. Katal. (Eng. transl.)*, **1978**, *19*, 1265.

Nonnegligible Dynamical Consequences of Vibration-Pseudorotation Coupling in a Symmetric Triatomic Molecule

Jae Shin Lee

Department of Chemistry, College of Natural Sciences,
Ajou University, Suwon 441-749, Korea

Received May 3, 1995

It is well known that vibration-rotation interaction becomes an important factor for understanding the spectra and dynamical behavior in polyatomic molecules as the total angular momentum of the system increases.¹⁻⁴ For the states with zero total angular momentum, it is generally assumed that vibration-rotation coupling is very negligible and most treatments on vibration-rotation interaction usually ignore the effect of coupling terms in the kinetic energy operator.^{5,6} How-

ever, there has been no systematic investigation on the effects of these coupling terms on the dynamics of polyatomic molecules as the molecular vibrational energy goes into higher regime. Since the angular momentum of the system can also be induced by the simultaneous vibrations, there could exist a coupling between vibration and rotation even for so called "rotationless" states ($J=0$) and the coupling effect may not be negligible in some highly excited levels. In this report, we present the case for which vibration-rotation coupling for $J=0$ (which will be called vibration-pseudorotation coupling) plays a nonnegligible role in destroying regular mode structure of the vibrational wavefunction in triatomic molecules.

The theoretical method and technique employed in this study were presented in detail in previous paper.⁷ In short, the vibration-rotation Hamiltonian for a symmetric triatomic molecule derived in arbitrary mode coordinate⁸ was used with the model potential function which can represent the real molecular potential surfaces reasonably. The Hamiltonian then was divided by pure vibrational (unperturbed) part and vibration-rotation coupling (perturbation) part. Therefore, the Hamiltonian operator was written as

$$H = H_0 + T_{V-R}$$

where H_0 is pure vibrational Hamiltonian including potential and T_{V-R} represents the coupling between vibration and rotation in the kinetic energy operator. The model potential function for a symmetric triatomic molecule with slight barrier to linearity was devised in Ref. 9 and developed further to include important coupling terms between vibrational modes in the expansion. In our case, the model potential function was expanded as

$$V(\eta_s, \eta_a, \eta_b) = c_s f_s^2 + c_a f_a^2 + x_1 f_b^2 + x_2 f_b^4 + x_3 f_b^6 + e f_s f_a^2$$

The stretching coefficients, c_s and c_a , are given initially with

Table 1. Expansion coefficients for the model potential function of an ABA triatomic molecule

$$V(\eta_s, \eta_a, \eta_b) = c_s f_s^2 + c_a f_a^2 + x_1 f_b^2 + x_2 f_b^4 + x_3 f_b^6 + e f_s f_a^2$$

$$f_i = \frac{\tanh(a_i \eta_i)}{a_i}; \quad i = a, b \quad f_i = \frac{1 - \exp(-a_i \eta_i)}{a_i}; \quad i = s$$

atomic mass	$m_A = \text{mass of } ^1\text{H}, m_B = \text{mass of } ^{12}\text{C}$
potential parameter	$a_s = 0.8 \quad a_b = 6.0 \quad a_a = 1.4$
reference configuration ^a	$r^0 = 1.065 \text{ \AA} \quad \theta_0 = 180^\circ$
equilibrium configuration ^b	$r_e = 1.070 \text{ \AA} \quad \theta_e = 136^\circ$
barrier height to linearity	1000 cm^{-1}

expansion coefficients^c

c_s	0.3484798
c_a	65.17453
x_1	-2.965045
x_2	1364.669
x_3	35.06913
ϵ	-52.19362

^a r^0 is the bond length between atom B and atom A in the linear saddle point geometry defined in Ref. 5. ^b r_e is the equilibrium bond length between atom B and atom A. ^c In units of hartree/(\AA^n), where $n=2$ for c_s, c_a, x_1 ; $n=4$ for x_2 ; and $n=3$ for x_3, ϵ .